 doi:10.20944/preprints202107.0292.v2

Article

ANTIBIOTIC REMOVAL FROM AQUATIC ENVIRONMENT WITH ACTIVATED CARBON PRODUCED FROM THE PUMPKIN SEEDS

İhsan Alacabey [1,*]

[1] ihsanalacabey@hotmail.com; ihsanalacabey@artuklu.edu.tr
* Correspondence: e-mail@e-mail.com; Tel.: (optional; include country code; if there are multiple corresponding authors, add author initials)

Abstract: Antibiotics are among the most critical environmental pollutant drug groups. One of the methods used to remove this pollution is adsorption. In this study, activated carbon was produced from the pumpkin seed shell and then modified with KOH. This adsorbent obtained was used in the removal of ciprofloxacin from aqueous systems. Fourier Transform-Infrared Spectroscopy (FT-IR), Scanning Electron Microscopy (SEM), elemental, X-ray Photoelectron Spectroscopy (XPS), Brunauer-Emmett-Teller (BET) and Zeta analyzes were used for the characterization of the adsorbent. In particular, the surface area was found to be a very remarkable value of 2730 m^2/g. The conditions of the adsorption experiments were optimized based on interaction time, adsorbent amount, pH and temperature. Over 99% success has been achieved in removal works carried out under the most optimized conditions. In addition, it was determined that the Langmuir isotherm is the most suitable model for the adsorption interaction

Keywords: Activated carbon, adsorption, ciprofloxacin, pollutant, pumpkin seed, thermodynamics.

1. Introduction

Pharmaceutical drugs have been known as hazardous class contaminants due to their comprehensive and long-dated active mechanism on the aquatic aqueous system. Antibiotics are the name given to a group of drugs used to treat infections caused by sundry microbes, such as bacteria and some parasites [1, 2]. Approximately 30-90% of the amount of antibiotic taken into the organism can remain intact in humans or animals, and it is also actively eliminated from the body [3]. The presence of antibiotics in the environment can trigger antibiotic-resistant bacteria's growth even at low concentrations, harming ecological life [4]. Fluoroquinolone (FQ) antibiotics are very popular in the medical and veterinary fields [5]. Ciprofloxacin (CIP) is one of the widely preferred FQ antibiotics in the World [6]. This antibiotic has been measured in streams and wastewater influents and effluents at concentrations typically <1 μg L^{-1}; however, higher concentrations have been measured in wastewater from hospitals (3-87 μg L^{-1}) and drug manufacturing facilities (31 mg L^{-1}) [7]. Therefore, the disposal of CIP residues from the environment is a vital topic.

Many applications have been used to treat effluents rich in FQs, such as electrochemical oxidation [8], biodegradation [9], photodegradation [10], catalytic degradation [11], micro-extraction [12], oxidation (catalytic degradation) [13] and adsorption [14]. From current methods, adsorption has proven to be a easy, high-performance and cheap technique to remove low concentration FQ contaminants from aqueous medium [15]. Adsorption is a overused practice for removing a wide variety of FQ contaminants due to its simple plannig, practical handling, and relatively effortless regeneration. Activated carbon is a generic term for a family of highly porous, amorphous carbon materials [16]. It is a useful

Preprints (www.preprints.org) | NOT PEER-REVIEWED | Posted: 14 July 2021 doi:10.20944/preprints202107.0292.v2

adsorbent in removing FQs compared to zeolite [17], clay [18], silica [19] and carbon nanotube [20] due to its extensive surface area, microporous structure and superior adsorption capacity [21]. However, Its high cost prevents its widespread use. For this reason, low-cost alternative methods of carbon preparation are being investigated and plant-based wastes come to the fore in this regard.

Pumpkin is one of the most important vegetables grown around the World. It is a gourd-like squash and belongs to the Cucurbitaceae family. Pumpkin seeds, also known as pepitas, are flattened and variable in size, shape, and colour. Pumpkin seeds have been used to extract the oil, which has various benefits such as anti-microbial, anti-fungal and anti-viral properties [22]. As a potential adsorbent, the pumpkin seed shell survey shows many researchers are working on its preparation and use for contaminant removal [23-26].

In this study, KOH modified pumpkin seed shell was used to remove CIP drug from aqueous systems. The aim here is to show that activated carbon obtained from pumpkin seed shell can effectively remove drug waste from aqueous systems. In practical applications using batch system adsorption technique, adsorption conditions were optimized in terms of adsorbent amount, interaction time, pH and temperature.

2. MATERIAL and METHOD

2.1. Material

2.2. Preparation of the Adsorbent

First, the raw sample was carbonized for one hour by applying a heating rate of 10 °C/min at 500 °C. The charred sample was mixed with KOH in the presence of sufficient water and dried. The dried sample was activated by nitrogen for one hour at 800 °C (heating rate 10 °C/min). After removing the sample from the oven, it was cooled to room temperature and washed with dilute HCl until defoaming by heating with water. It was then washed with distilled water for chlorine testing. Finally, the sample was ground and stored in plastic containers.

2.3. Characterization of the Adsorbent

Fourier Transform-Infrared Spectroscopy (FT-IR) analysis was performed to prove that the activated carbon obtained from the pumpkin seed shell was functionalized with KOH. Scanning Electron Microscopy (SEM) analysis was used to examine the morphological structure of the adsorbent in detail. Also, the elemental analysis technique was applied to determine the elemental composition of the adsorbent. Besides, the net load of the adsorbent was determined by Zeta analysis. X-ray Photoelectron Spectroscopy (XPS) was also used for measuring the elemental composition of the surface of the material, and it also determines the binding states of the elements. At the same time, BET (Brunauer-Emmett-Teller) analysis was performed to determine the surface area of the adsorbent.

2.4. Adsorption Studies

Batch system was preferred for CIP removal from aqueous systems. Adsorption studies were carried out according to the interaction time, adsorbent amount, pH and temperature parameters. Afterwards, practical applications continued under optimized conditions. UV-VIS spectrometer (UV-VIS 754, CHINA) was used to determine the amount of CIP before and after adsorption and was studied at 275 nm wavelength [27]. The calculation of the adsorption (%) was made according to the following equation.

$$\text{Adsorption } (\%) = \frac{(C_0 - C_e)}{C_o} x\ 100 \quad \text{(Eq 1)}$$

Preprints (www.preprints.org) | NOT PEER-REVIEWED | Posted: 14 July 2021 doi:10.20944/preprints202107.0292.v2

In Equation 1, C_o: is the starting concentration of CIP in solution (mg/L); C_e: final CIP concentration in solution (mg/L).

Within the scope of adsorption works, interaction time study was performed first. Measurements were taken in the period of 1-90 min, and the sample was taken in a volume of 1.5 mL each time and centrifuged at 3000 rpm. Then the focus was on the optimum amount of adsorbent (5-50 mg). For the pH study, experimental applications were carried out in the range of 3.0-9.0. Finally, adsorption experiments were carried out at three different temperatures (15, 30, 45 °C) under pre-determined optimum conditions.

3. RESULTS

3.1. Characterization

The effect of the CIP adsorption on the IR spectra is shown in Figure 1. The spectra of bare activated carbon and CIP adsorbed activated carbon were examined, and no significant difference was detected. In both spectra, in the range of 3450–3700 cm^{-1}, the band derived from the group –OH is visible. The C–H bending vibration and C–O stretching peaks (2700-3000, 1250-1500, 500-700 cm^{-1}) should be especially highlighted. The peak at 1690 cm^{-1} can occur from the C=C group. However, it was observed that the intensity of the C-H bands in the spectrum of CIP adsorbed activated carbon was higher. This may be due to CIP adsorbed on the structure.

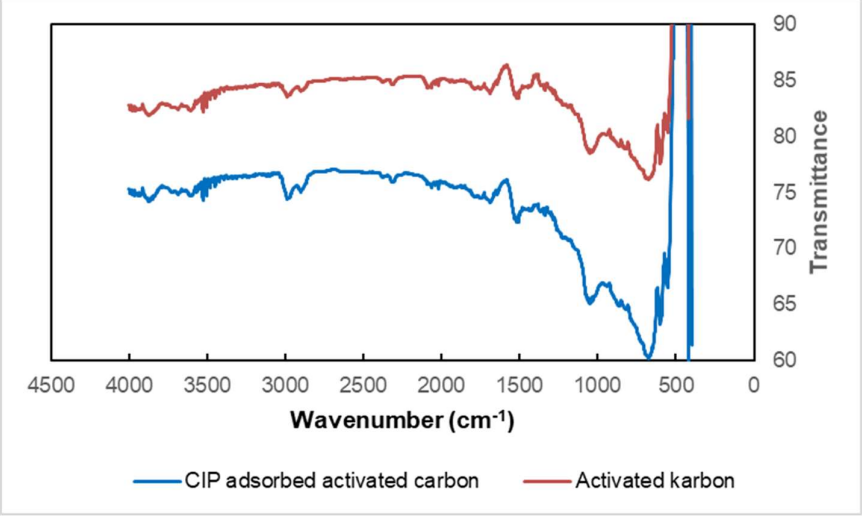

Figure 1. FT-IR spectra of activated carbons.

When the SEM analysis of the adsorbent is examined, it is particularly striking that it has a porous structure (Figure 2). The porous structure of construction is considered an essential advantage for adsorption [28-32].

Preprints (www.preprints.org) | NOT PEER-REVIEWED | Posted: 14 July 2021 doi:10.20944/preprints202107.0292.v2

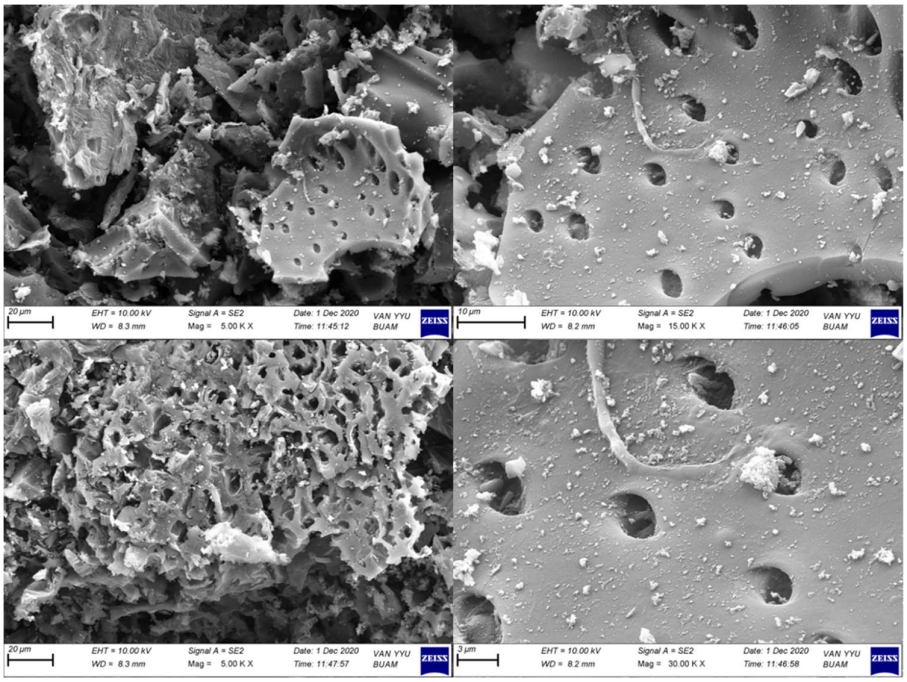

Figure 2. SEM images of modified activated carbon.

Elemental analysis results of the adsorbent are given in Table 1. The remarkable detail from the data obtained is that the sum of the elements carbon, hydrogen, nitrogen and sulfur constitutes approximately 98.5% of the total mass. This result can be interpreted as that 1.5% of the total mass can be composed of potassium and oxygen elements.

Table 1. Elemental analysis results of the adsorbent

Element Name	Amount
Nitrogen	1.2331
Carbon	96.9629
Hydrogen	0.313
Totals	98.509

XPS studied the chemical composition of the surface. The identification of potassium as well as the carbon atom in the spectrum is interpreted as a result of the KOH treatment on the adsorbent (Figure 3).

Preprints (www.preprints.org) | NOT PEER-REVIEWED | Posted: 14 July 2021 doi:10.20944/preprints202107.0292.v2

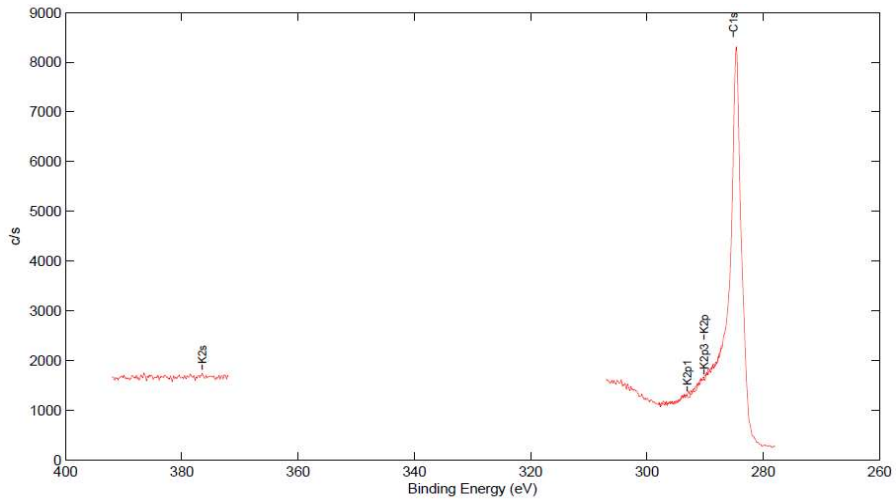

Figure 3. XPS spectrum of KOH modified activated carbon.

As a result of Zeta analysis, the potential of the adsorbent at pH: 8.0 was calculated as 18.5 mV. In addition, it was determined that the isoelectric point of the adsorbent was 9.41. Accordingly, at the pH: 9.41 point, the adsorbent is uncharged, it is positive at the points below this value and negatively charged at the points above it. At the end of BET analysis, the surface area of the adsorbent was found to be 2729.7 m2/g. This value is enormously high, and it is proof that the adsorption ability of the adsorbent is very high. Such a high surface area value has not been found among the studies examined in the literature. This result is, therefore, one of the most prominent parameters of this study.

3.2. Adsorption

In studies aimed at optimizing the adsorption conditions, first, the optimum interaction time was determined. The results of the adsorption experiments conducted in the range of 1-90 minutes are presented in Figure 4. As can be seen, until the 45th minute, the amount of CIP adsorbed increased significantly, but after this minute, no significant increase was observed in the amount of CIP adsorbed. The reason for this situation is that the adsorption regions of the adsorbent are completely filled with CIP. The study conducted to determine the optimum adsorbent amount shows that the adsorption rate was almost fixed after 20 mg of adsorbent amount (Figure 5). At this point, nearly all of the CIP in the environment was adsorbed by active carbon. For this reason, 20 mg of activated carbon was determined as the most suitable adsorbent amount. In adsorption studies carried out at different pH values, the highest adsorption rate was reached at pH: 8.0 point (Figure 6). The charge distribution between activated carbon and CIP changes with the change of pH value of the environment, and the most effective interaction is provided at this point. Besides, CIP adsorption at different concentrations was carried out at three different temperatures (Figure 7). As can be seen from the graph, the rate of CIP removal increased as the temperature increased in the adsorption applications with the same concentration of the solution. Accordingly, it can be said that the interactions that are effective for adsorption are non-ionic interactions (hydrophobic).

Preprints (www.preprints.org) | NOT PEER-REVIEWED | Posted: 14 July 2021 doi:10.20944/preprints202107.0292.v2

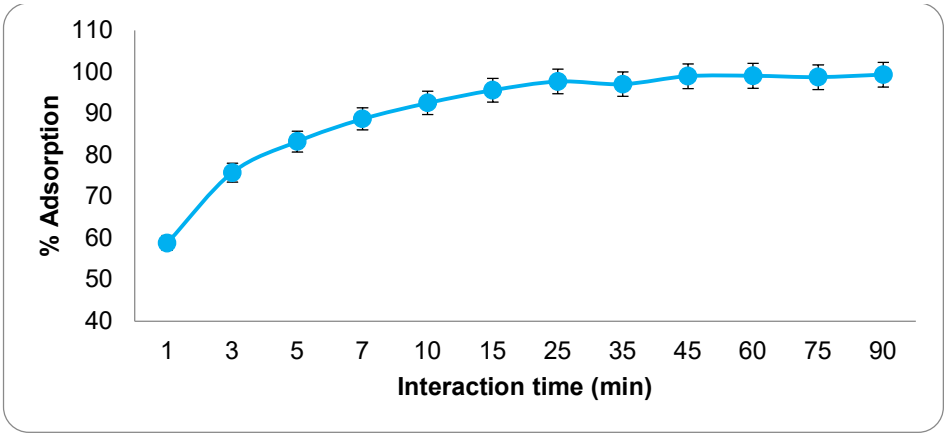

Figure 4. The effect of interaction time on the amount of adsorption. (CCIP: 40 mgL^{-1}, adsorbent amount: 37.5 mg, temperature: 30 °C)

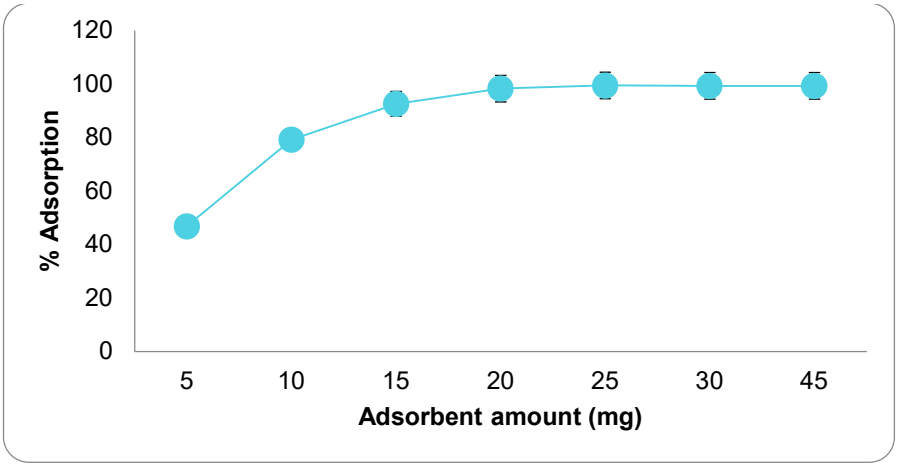

Figure 5. The effect of the amount of adsorbent on adsorption. (CCIP: 100 mgL^{-1}, interaction time: 45 min, temperature: 30 °C)

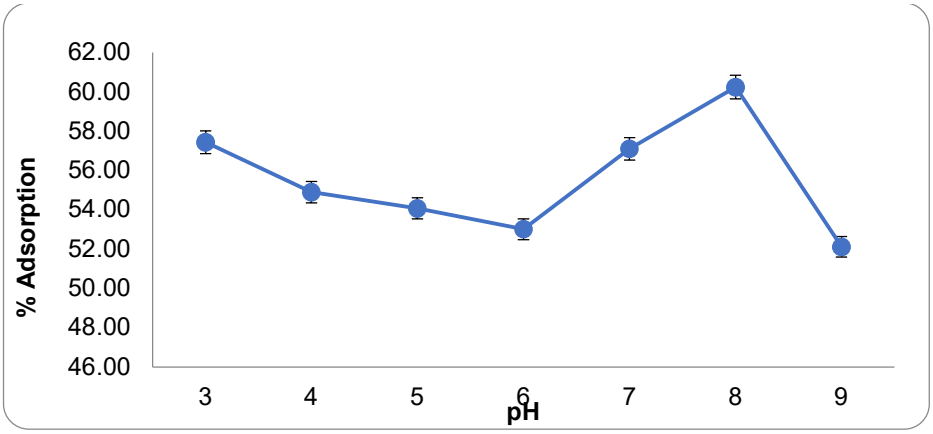

Figure 6. The effect of pH change on adsorption. (CCIP: 300 mgL^{-1}, interaction time: 45 min, adsorbent amount: 20.0 mg, temperature: 30 °C)

Preprints (www.preprints.org) | NOT PEER-REVIEWED | Posted: 14 July 2021 doi:10.20944/preprints202107.0292.v2

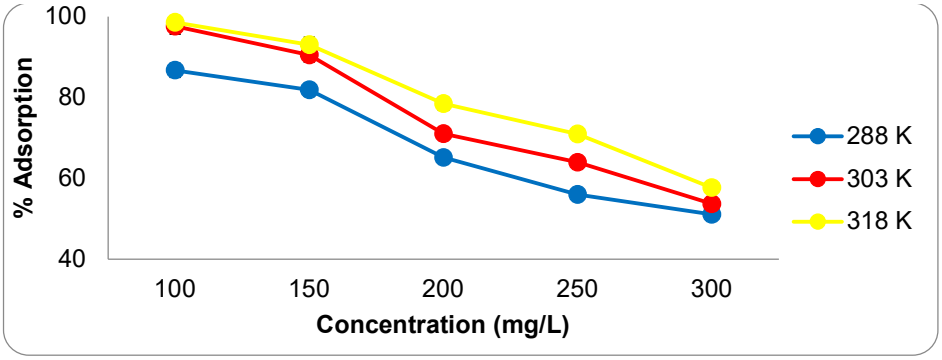

Figure 7. Effect of temperature change on adsorption. (Interaction time: 45 min, adsorbent amount: 20.0 mg, pH: 8.0)

3.3. Isotherm and Kinetics

Linear adsorption isotherm models [Freundlich, Langmuir-1, Langmuir-2, Langmuir-3, Langmuir-4, Langmuir-5, Temkin ve Dubinin–Radushkevich (D-R)] were used to explain the structure (surface properties, adsorption mechanism and capacity) of CIP adsorption on active carbon at 288, 303 and 313 K. The equations and parameters of the linear isotherm models used, are shown in Table 2 together with the relevant references [33-36].

Equilibrium data were applied to the five linear Langmuir isotherm model equations and the Linear Freundlich isotherm model. The equilibrium data and the Langmuir-1 isotherm model showed a high correlation (R^2) (Table 2). The Langmuir model assumes homogeneous adsorption energies to the surface, and there is no adsorbate transition on the surface plane [34, 37-44]. The Langmuir equation can be written as:

$$q_e = \frac{C_e b C_e}{1+bC_e} \qquad \text{(Eq 2)}$$

CIP's adsorption data on active carbon were analyzed to fit five linearized expressions of the Langmuir isotherm model. Details of these five different forms of linearized Langmuir equations and the values of Langmuir constants q_m and b are explained in Table 2. Among the correlation coefficient values of five different types of linearized Langmuir isotherm equations, Langmuir-1 was the most appropriate. Maximum adsorption capacity values determined using Langmuir-1 expression are higher than experimentally adsorbed amounts and correspond to adsorption isotherm plateaus. On the contrary, according to the single-layer adsorption capacities and correlation coefficients obtained by using the other four linear expressions of the Langmuir model, it is seen that the Langmuir-1 isotherm better matches the experimental Data [34]. This result shows that adsorption takes place in a single layer and is homogeneous [45, 46].

Freundlich's constant (K_F) depending on the adsorption capacity ranged from 265.58 mg/g to 418.56 mg/g with the temperature range studied. The value of K_F increased with increasing temperature, which means that the adsorption interaction is endothermic. The n value is a constant that determines the type of process: If n = 1, adsorption is linear; If n <1, adsorption is a chemical process; If n> 1, adsorption is a physical process. From Table 2, the 1/n value is 0.2152, 0.2079 and 0.1736 at 288, 303, and 318 K, respectively. So, the n value in this study was determined as 4.6472, 4.8094, 5.7614 for all temperatures examined. The n>1 case is the most common. It can be caused by any factor that causes the distribution of surface areas or a decline in the adsorbent-adsorbate interaction with increased surface density. Values in the range 1-10 represent proper CIP adsorption and physical adsorption on active carbon [47].

 doi:10.20944/preprints202107.0292.v2

According to the Temkin isotherm, the decrease in the heat of adsorption of all molecules occurs in a linear order. This indicates that the binding energy is homogeneous. [48]. While the typical binding energy range for the ion exchange mechanism is reported to be in the 8-16 kJ/mol range, the adsorption energies of physical absorption processes are said to be less than −40 kJ/mol. The shallow b values (0.0190 - 0.0222 kJ/mol) obtained in the present study show a weak ionic interaction between the sorbate and the existing sorbent, and removal of CP appears to involve physisorption [49].

The Langmuir and Freundlich isotherms are insufficient to clarify the physical and chemical properties of adsorption. The D-R isotherm is more general than the Langmuir isotherm because it does not assume a homogeneous surface or a constant sorption potential [50]. Average adsorption energy (E) gives information about chemical and physical adsorption. When the size of E <8 kJmol^{-1}, the adsorption process is physical adsorption, and when E is between 8 kJmol−1 and 16 kJmol^{-1}, the process is chemical adsorption [51]. As seen in Table 2, the adsorption interaction is physical since the E value is <8 kJmol^{-1}.

Table 2. Isotherm models

Preprints (www.preprints.org) | NOT PEER-REVIEWED | Posted: 14 July 2021 doi:10.20944/preprints202107.0292.v2

Isotherm	Linear form	Constants	Temp.	Constant parameters			
Freundlich	$lnq_e = lnK_F + \frac{1}{n} lnC_e$	K_F (Lmg^{-1}): Adsorption capacity. n: Heterogeneity factor.		**n**	**1/n**	**K_F (mg/g)**	**R^2**
			288	4.6472	0.2152	265.58	0.8732
			303	4.8094	0.2079	311.35	0.8902
			318	5.7614	0.1736	418.56	0.9470
Langmuir - 1	$\frac{1}{q_e} = \left(\frac{1}{bq_m}\right)\frac{1}{C_e} + \frac{1}{q_m}$	q_m (mgg^{-1}): Maximum adsorption capacity. b (Lmg^{-1}): the constant related to the free energy of adsorption.		**b (L/mg)**	**q_m (mg/g)**	**R^2**	
			288	0.0836	804.88	0.9940	
			303	0.2781	819.61	0.9972	
			318	0.4176	884.90	0.9983	
Langmuir - 2	$\frac{C_e}{q_e} = \frac{1}{q_m} C_e + \frac{1}{bq_m}$	q_m (mgg^{-1}): Maximum adsorption capacity. b (Lmg^{-1}): the constant related to the free energy of adsorption.		**B (L/mg)**	**q_m (mg/g)**	**R^2**	
			288	0.0951	792.56	0.9537	
			303	0.7119	774.08	0.9598	
			318	1.0181	832.22	0.9502	
Langmuir - 3	$q_e = q_m - \left(\frac{1}{b}\right)\frac{q_e}{C_e}$	q_m (mgg^{-1}): Maximum adsorption capacity. b (Lmg^{-1}): the constant related to the free energy of adsorption.		**b (L/mg)**	**q_m (mg/g)**	**R^2**	
			288	0.1013	784.18	0.8899	
			303	0.6941	777.83	0.9119	
			318	0.9797	838.99	0.8881	
Langmuir - 4	$\frac{q_e}{C_e} = bq_m - bq_e$	q_m (mgg^{-1}): Maximum adsorption capacity. b (Lmg^{-1}): the constant related to the free energy of adsorption.		**b (L/mg)**	**q_m (mg/g)**	**R^2**	
			288	0.0901	802.84	0.8899	
			303	0.6329	785.65	0.4683	
			318	0.8701	850.73	0.8881	
Langmuir - 5	$\frac{1}{C_e} = bq_m\frac{1}{q_e} - b$	q_m (mgg^{-1}): Maximum adsorption capacity. b (Lmg^{-1}): the constant related to the free energy of adsorption.		**b (L/mg)**	**q_m (mg/g)**	**R^2**	
			288	0.0894	804.28	0.9537	
			303	0.6790	778.93	0.9379	
			318	0.9588	839.61	0.9502	
Temkin	$q_e = B_T lnK_T + B_T lnC_e$ $B_T = (RT)/b$	B_T ($Jmol^{-1}$): Adsorption heat. K_T (Lmg^{-1}): Temporal coefficient and adsorption capacity. T (K): Absolute temperature. R: Universal gas constant (8.314 $JK^{-1}mol^{-1}$).		**b (kj/mol)**	**Kt (L/mg)**	**R^2**	
			288	0.0190	2.9322	0.9043	
			303	0.0192	4.5938	0.9264	
			318	0.0222	22.1366	0.9754	
Dubinin–Radushkevich	$lnq_e = lnq_m - \beta\varepsilon^2$ $\varepsilon = RTln\left[1 + \frac{1}{C_e}\right]$ $E_\alpha = \left[\frac{1}{\sqrt{2\beta}}\right]$	q_m (mgg^{-1}): D – R adsorption capacity. β (mol^2kJ^{-2}): Adsorption average free energy coefficient. ε (kJ^2/mol^2): Polanyi adsorption potential.		**q_m (mol/g)**	**E (kj/mol)**	**R^2**	
			288	717.2100	0.1622	0.9424	
			303	780.3484	0.2427	0.9430	
			318	836.7270	0.6597	0.8905	

Preprints (www.preprints.org) | NOT PEER-REVIEWED | Posted: 14 July 2021 doi:10.20944/preprints202107.0292.v2

		E_a (kJmol^{-1}): D-R adsorption free energy. T (K): Absolute temperature. R : Universal gas constant (8.314 JK−1mol−1).		

The thermodynamic behaviour of CIP adsorption on active carbon was evaluated using the ΔG°, ΔH° and ΔS° (entropy change) [35]. In order to find the Gibbs free energy of the adsorption process performed at a certain temperature, first the equilibrium constant Kc is calculated with the help of equation 3.

$$Kc = Ca / Ce \quad \text{(Eq 3)}$$

K_c : Equilibrium constant
C_a : Concentration of substance retained by the adsorbent (mg/L)
C_e : Concentration of residual substance in solution (mg/L)

$$\Delta G^0 = -R\ T\ \ln Kc \quad \text{(Eq 4)}$$

$$\ln K_c = \frac{\Delta S^o}{R} - \frac{\Delta H^o}{RT} \quad \text{(Eq 5)}$$

Here, R (8.314 Jmol $^{-1}$K $^{-1}$) is the ideal gas constant, and T (K) is the temperature at Kelvin. ΔHo is the enthalpy change, and ΔS^o is the entropy change in a given process.

If Kc, found with the help of Equation 3, is replaced in Equation 4, the Gibbs free energy of adsorption is found.

Using Equation 5, ΔH^o is calculated from the slope of the line formed by plotting the lnKc value against the 1/T value, and ΔS^o from the cut-off point. The values of ΔG° and ΔH°, ΔS° for CIP adsorption on activated carbon are given in Table 3.

Table 3. Thermodynamic data for CIP adsorption

C_0	ΔH°, kj/mol	ΔS°, j/mol	ΔG°, kj/mol		
			288 K	303 K	313 K
100	39.39	150.87	-4.34	-5.72	-8.93
150	25.71	101.54	-3.63	-4.84	-6.70
200	18.77	70.14	-1.53	-2.27	-3.66
250	16.43	59.14	-0.61	-1.45	-2.39
300	9.62	33.85	-0.16	-0.58	-1.18

It can be observed from Table 3 that the values of ΔH° are positive, indicating that the adsorption reaction is endothermic [49, 52, 53]. Negative ΔG° values indicate the degree of the spontaneity of the adsorption process, and a more negative value indicates an energetically positive adsorption process. The decrease in ΔG° with increasing temperature showed that adsorption at high temperature is more suitable. The value of G° was found negative for the adsorption of CIP on activated carbon at all temperatures, confirming the applicability of this adsorbent and the spontaneity of the adsorption process [49].

4. CONCLUSION

Within the scope of the study, CIP removal from aqueous systems with activated carbon obtained from pumpkin seed shell was achieved at a very high rate. The fact that the adsorbent has a very high surface area has been one of the most outstanding points in terms of work. It was determined that the adsorption interaction, which was made more efficient with optimization studies, fit the Langmuir model. Accordingly, we can say that CIP adsorption on activated carbon occurred as homogeneous and single layer. When the thermodynamic data obtained are examined, it is seen that adsorption takes place under the influence of physical forces. As a result, it can be said that the present adsorbent is a suitable material for CIP removal from aqueous media.

References

1. Darweesh, T.M. and M.J. Ahmed, *Adsorption of ciprofloxacin and norfloxacin from aqueous solution onto granular activated carbon in fixed bed column.* Ecotoxicology and environmental safety, 2017. **138**: p. 139-145.
2. Ashfaq, M., et al., *Occurrence and ecological risk assessment of fluoroquinolone antibiotics in hospital waste of Lahore, Pakistan.* Environmental toxicology and pharmacology, 2016. **42**: p. 16-22.
3. Pouretedal, H. and N. Sadegh, *Effective removal of amoxicillin, cephalexin, tetracycline and penicillin G from aqueous solutions using activated carbon nanoparticles prepared from vine wood.* Journal of Water Process Engineering, 2014. **1**: p. 64-73.
4. Prutthiwanasan, B., C. Phechkrajang, and L. Suntornsuk, *Fluorescent labelling of ciprofloxacin and norfloxacin and its application for residues analysis in surface water.* Talanta, 2016. **159**: p. 74-79.
5. Van Doorslaer, X., et al., *Fluoroquinolone antibiotics: an emerging class of environmental micropollutants.* Science of the Total Environment, 2014. **500**: p. 250-269.
6. Sun, Y., et al., *Characterization and ciprofloxacin adsorption properties of activated carbons prepared from biomass wastes by H3PO4 activation.* Bioresource Technology, 2016. **217**: p. 239-244.
7. Carabineiro, S., et al., *Comparison between activated carbon, carbon xerogel and carbon nanotubes for the adsorption of the antibiotic ciprofloxacin.* Catalysis Today, 2012. **186**(1): p. 29-34.
8. Zhu, L., et al., *Electrochemical oxidation of fluoroquinolone antibiotics: Mechanism, residual antibacterial activity and toxicity change.* Water Research, 2016. **102**: p. 52-62.
9. Čvančarová, M., et al., *Biotransformation of fluoroquinolone antibiotics by ligninolytic fungi–Metabolites, enzymes and residual antibacterial activity.* Chemosphere, 2015. **136**: p. 311-320.
10. Sturini, M., et al., *Sunlight-induced degradation of fluoroquinolones in wastewater effluent: Photoproducts identification and toxicity.* Chemosphere, 2015. **134**: p. 313-318.
11. Feng, M., et al., *Degradation of fluoroquinolone antibiotics by ferrate (VI): Effects of water constituents and oxidized products.* Water Research, 2016. **103**: p. 48-57.
12. Ebrahimpour, B., Y. Yamini, and M. Moradi, *Application of ionic surfactant as a carrier and emulsifier agent for the microextraction of fluoroquinolones.* Journal of Pharmaceutical and Biomedical Analysis, 2012. **66**: p. 264-270.
13. Guo, H., et al., *Kinetics and transformation pathways on oxidation of fluoroquinolones with thermally activated persulfate.* Chemical Engineering Journal, 2016. **292**: p. 82-91.
14. Ferreira, V.R., et al., *Fluoroquinolones biosorption onto microbial biomass: activated sludge and aerobic granular sludge.* International Biodeterioration & Biodegradation, 2016. **110**: p. 53-60.
15. Tan, F., et al., *Preparation of molecularly imprinted polymer nanoparticles for selective removal of fluoroquinolone antibiotics in aqueous solution.* Journal of Hazardous Materials, 2013. **244**: p. 750-757.
16. Depci, T., et al., *Characteristic properties of adsorbed catalase onto activated carbon based adiyaman lignite.* Fresenius Environmental Bulletin, 2011. **20**(9A): p. 2371-2378.

17. Maraschi, F., et al., *TiO2-modified zeolites for fluoroquinolones removal from wastewaters and reuse after solar light regeneration.* Journal of Environmental Chemical Engineering, 2014. **2**(4): p. 2170-2176.
18. Sturini, M., et al., *Removal of fluoroquinolone contaminants from environmental waters on sepiolite and its photo-induced regeneration.* Chemosphere, 2016. **150**: p. 686-693.
19. Liang, Z., et al., *Adsorption of quinolone antibiotics in spherical mesoporous silica: Effects of the retained template and its alkyl chain length.* Journal of Hazardous Materials, 2016. **305**: p. 8-14.
20. Yu, F., et al., *Adsorptive removal of antibiotics from aqueous solution using carbon materials.* Chemosphere, 2016. **153**: p. 365-385.
21. Ahmed, M.J. and S.K. Theydan, *Fluoroquinolones antibiotics adsorption onto microporous activated carbon from lignocellulosic biomass by microwave pyrolysis.* Journal of the Taiwan Institute of Chemical Engineers, 2014. **45**(1): p. 219-226.
22. Almaz Kemal, K.S., Wondmagegn H. Michael, *Adsorption of Cu (II) and Cd (II) onto Activated Carbon Prepared from Pumpkin Seed Shell.* Journal of Environmental Science and Pollution Research, 2019. **5**(1): p. 328-333.
23. Demiral, İ. and C.A. Şamdan, *Preparation and characterisation of activated carbon from pumpkin seed shell using H3PO4.* Anadolu Üniversitesi Bilim ve Teknoloji Dergisi A-Uygulamalı Bilimler ve Mühendislik, 2016. **17**(1): p. 125-138.
24. Kuśmierek, K., A. Świątkowski, and L. Dąbek, *Removal of 2, 4, 6-trichlorophenol from aqueous solutions using agricultural waste as low-cost adsorbents.* Environment Protection Engineering, 2017. **43**(4).
25. Demiral, İ., T. Bektaş, and C. Şamdan, *Utilization of activated carbon prepared from pumpkin seed shell for the removal of dyestuff from aqueous solutions and wastewater by microwave radiation.* International Journal of Scientific and Technological Research, 2019. **5**(2): p. 68-77.
26. Demiral, I., C. Aydın Şamdan, and H. Demiral, *Production and characterization of activated carbons from pumpkin seed shell by chemical activation with ZnCl2.* Desalination and Water Treatment, 2016. **57**(6): p. 2446-2454.
27. Cazedey, E.C.L. and H.R.N. Salgado, *Spectrophotometric determination of ciprofloxacin hydrochloride in ophthalmic solution.* Advances in Analytical Chemistry, 2012. **2**(6): p. 74-79.
28. Erol, K. and L. Uzun, *Two-step polymerization approach for synthesis of macroporous surface ion-imprinted cryogels.* Journal of Macromolecular Science, Part A, 2017. **54**(11): p. 867-875.
29. Erol, K., et al., *Synthesis, characterization and antibacterial application of silver nanoparticle embedded composite cryogels.* Journal of Molecular Structure, 2020. **1200**: p. 127060.
30. Erol, K., et al., *Antimicrobial magnetic poly (GMA) microparticles: synthesis, characterization and lysozyme immobilization.* Journal of Polymer Engineering, 2020. **41**(2): p. 144-154.
31. Erol, K., *Synthesis, Characterization and Chromatographic Applications of Antimicrobial Cryogels.* Hacettepe Journal of Biology and Chemistry, 2017. **45**(2): p. 187-195.
32. Ece, M.Ş., *Synthesis and characterization of activated carbon supported magnetic nanoparticles (Fe3O4/AC@ SiO2@ Sulfanilamide) and its application in removal of toluene and benzene.* Colloids and Surfaces A: Physicochemical and Engineering Aspects, 2021. **617**: p. 126231.
33. Acet, Ö., et al., *O-carboxymethyl chitosan Schiff base complexes as affinity ligands for immobilized metal-ion affinity chromatography of lysozyme.* Journal of Chromatography A, 2018. **1550**: p. 21-27.
34. Hamdaoui, O. and E. Naffrechoux, *Modeling of adsorption isotherms of phenol and chlorophenols onto granular activated carbon: Part I. Two-parameter models and equations allowing determination of thermodynamic parameters.* Journal of Hazardous Materials, 2007. **147**(1-2): p. 381-394.
35. Banerjee, P., et al., *Optimization and modelling of synthetic azo dye wastewater treatment using graphene oxide nanoplatelets: characterization toxicity evaluation and optimization using artificial neural network.* Ecotoxicology and Environmental Safety, 2015. **119**: p. 47-57.

36. Wakkel, M., B. Khiari, and F. Zagrouba, *Basic red 2 and methyl violet adsorption by date pits: adsorbent characterization, optimization by RSM and CCD, equilibrium and kinetic studies.* Environmental Science and Pollution Research, 2019. **26**(19): p. 18942-18960.
37. Erol, K., *The adsorption of calmoduline via nicotinamide immobilized poly (HEMA-GMA) cryogels.* Journal of the Turkish Chemical Society Section A: Chemistry, 2017. **4**(1): p. 133-148.
38. Erol, K., *Polychelated cryogels: hemoglobin adsorption from human blood.* Artificial Cells, Nanomedicine, and Biotechnology, 2017. **45**(1): p. 31-38.
39. Erol, K., et al., *Magnetic diatomite for pesticide removal from aqueous solution via hydrophobic interactions.* Environmental Science and Pollution Research, 2019. **26**(32): p. 33631-33641.
40. Erol, K., *DNA adsorption via Co (II) immobilized cryogels.* Journal of Macromolecular Science, Part A, 2016. **53**(10): p. 629-635.
41. Erol, B., K. Erol, and E. Gökmeşe, *The effect of the chelator characteristics on insulin adsorption in immobilized metal affinity chromatography.* Process Biochemistry, 2019. **83**: p. 104-113.
42. Kireç, O., et al., *Removal of 17β-estradiol from aqueous systems with hydrophobic microspheres.* Journal of Polymer Engineering, 2021. **41**(3): p. 226-234.
43. Alacabey, İ., et al., *Pumice particle interface: a case study for immunoglobulin G purification.* Polymer Bulletin, 2020. (in press)
44. Tosun Satır, İ. and K. Erol., *Calcined Eggshell for the Removal of Victoria Blue R Dye from Wastewater Medium by Adsorption.* Journal of the Turkish Chemical Society, Section A: Chemistry, 2021. **8**(1): p. 47-56.
45. Alacabey, İ., et al., *Van gölü doğal sediment ve modifiye sediment üzerine krom (III) adsorpsiyonu (izoterm ve termodinamik analiz çalışması).* Dicle Üniversitesi Mühendislik Fakültesi Mühendislik Dergisi, 2020. **11**(3): p. 1225-1232 (in Turkish).
46. Ece, M.S.a., et al., *Development of novel Fe3O4/AC@ SiO2@ 1, 4-DAAQ magnetic nanoparticles with outstanding VOC removal capacity: characterization, optimization, reusability, kinetics, and equilibrium studies.* Industrial & Engineering Chemistry Research, 2020. **59**(48): p. 21106-21123.
47. Shin, H.S. and J.-H. Kim, *Isotherm, kinetic and thermodynamic characteristics of adsorption of paclitaxel onto Diaion HP-20.* Process Biochemistry, 2016. **51**(7): p. 917-924.
48. ALOthman, Z.A., M. Naushad, and R. Ali, *Kinetic, equilibrium isotherm and thermodynamic studies of Cr (VI) adsorption onto low-cost adsorbent developed from peanut shell activated with phosphoric acid.* Environmental Science and Pollution Research, 2013. **20**(5): p. 3351-3365.
49. Kiran, B. and A. Kaushik, *Chromium binding capacity of Lyngbya putealis exopolysaccharides.* Biochemical Engineering Journal, 2008. **38**(1): p. 47-54.
50. Caliskan, N., et al., *Adsorption of Zinc (II) on diatomite and manganese-oxide-modified diatomite: A kinetic and equilibrium study.* Journal of Hazardous Materials, 2011. **193**: p. 27-36.
51. Hu, Q. and Z. Zhang, *Application of Dubinin–Radushkevich isotherm model at the solid/solution interface: a theoretical analysis.* Journal of Molecular Liquids, 2019. **277**: p. 646-648.
52. Ngah, W.W. and S. Fatinathan, *Adsorption of Cu (II) ions in aqueous solution using chitosan beads, chitosan–GLA beads and chitosan–alginate beads.* Chemical Engineering Journal, 2008. **143**(1-3): p. 62-72.
53. Hu, X.-j., et al., *Adsorption of chromium (VI) by ethylenediamine-modified cross-linked magnetic chitosan resin: isotherms, kinetics and thermodynamics.* Journal of Hazardous Materials, 2011. **185**(1): p. 306-314.